Fractal Analysis of Deep Ocean Current Speed Time Series

LAURA CABRERA-BRITO

Departamento de Fisica, Universidad de Las Palmas de Gran Canaria, Las Palmas de Gran Canaria, Las Palmas, Spain

GERMAN RODRIGUEZ, LUIS GARCÍA-WEIL, MERCEDES PACHECO, AND ESTHER PEREZ

Applied Marine Physics and Remote Sensing Group, Institute of Environmental Studies and Natural Resources, and Departamento de Fisica, Universidad de Las Palmas de Gran Canaria, Las Palmas de Gran Canaria, Las Palmas, Spain

JOANNA J. WANIEK

Leibniz Institute for Baltic Sea Research, Rostock, Germany

(Manuscript received 24 May 2016, in final form 26 January 2017)

ABSTRACT

Fractal properties of deep ocean current speed time series, measured at a single-point mooring on the Madeira Abyssal Plain at 1000- and 3000-m depth, are explored over the range between one week and 5 years, by using the detrended fluctuation analysis and multifractal detrended fluctuation analysis methodologies. The detrended fluctuation analysis reveals the existence of two subranges with different scaling behaviors. Long-range temporal correlations following a power law are found in the time-scale range between approximately 50 days and 5 years, while a Brownian motion–type behavior is observed for shorter time scales. The multifractal analysis approach underlines a multifractal structure whose intensity decreases with depth. The analysis of the shuffled and surrogate versions of the original time series shows that multifractality is mainly due to long-range correlations, although there is a weak nonlinear contribution at 1000-m depth, which is confirmed by the detrended fluctuation analysis of volatility time series.

1. Introduction

A large portion of the total solar radiation incident on Earth's surface is absorbed and stored in the ocean, due to its relatively high heat capacity, where it is redistributed through ocean currents. In addition to seawater, ocean water masses may contain many other dissolved or suspended materials and living organisms. Therefore, ocean currents transport matter and energy from one part of the planet to another, representing a key factor in controlling Earth's climate and having important ecological implications. To an approximate degree, oceanic circulation can be separated into two modes with specific dynamics and time scales. In the upper layer, with a thickness ranging from approximately 500 to 1500 m (van Aken 2007; Pinet 2009), the more or less regular oceanic winds constitute the dominant process driving ocean currents, although density differences may also play a significant role. Below this layer circulation is mainly determined by density differences, resulting from regional differences in the exchange of heat and freshwater between atmosphere and ocean (Stewart 2009; Huang 2010). In reality, however, this is not a trivial distinction because both circulation modes are coupled.

The flow of water in the oceans is a result of the interaction among various nonlinear processes that take place across a wide range of space and time scales. In particular, temporal variability includes scales ranging from a few seconds out to millions of years (Huybers and Curry 2006). The complexity of the resulting process limits its proper understanding and hinders adequate characterization and prediction of ocean current speeds. Within this framework, a common and powerful approach used to gain insight into the dynamics governing the process is the analysis of time series, obtained by sampling the phenomenon under study, considered as a realization of a random process.

In this context, in addition to its probabilistic structure, a fundamental aspect to be considered for

Corresponding author e-mail: German Rodriguez, german.rodriguez@ulpgc.es

DOI: 10.1175/JTECH-D-16-0098.1

characterizing a random process, such as the ocean velocity field, is the correlation degree between values observed at different times, also known as persistence, which can be weak, strong, or null. Furthermore, correlation may exist between nearby values in the time series (short-range correlation) but also between values far away in the time sequence (long-range correlation).

Long-range dependence has been recognized, after the pioneering contributions of Mandelbrot and coworkers during the last part of the 1960s (see Mandelbrot and Wallis 1969 and references therein), as a characteristic feature of many phenomena, which provides insights into the underlying mechanisms that rule the process dynamics. Since then, the existence of long-range persistence has been established in a wide range of disciplines, including geophysical processes (Kantelhardt et al. 2003), network traffic modeling (Taqqu et al. 1997), economics (Mantegna and Stanley 1995), and physiology (Goldberger et al. 2002), among many others.

The analysis of possible long-range correlations, or temporal persistence, in time series helps to understand the natural variability of the process under study and its dynamics. Specifically, the existence of long-range correlations has important implications in terms of forecasting because scale invariance allows the relationship of variability between different time scales to be quantified (Bunde and Lennartz 2012). Furthermore, persistence implies that remote parts of the time series remain significantly correlated, and hence past events can have a notable effect on the present and future development of the process. So, long-range correlations play an important role in model assessment (Livina et al. 2007) and in understanding climate variability (Barbosa et al. 2006). Additionally, time series with persistent behavior exhibit positive and negative deviations from the average value for long periods. Hence, long-term persistence represents a natural mechanism that leads to the clustering of extreme events; therefore, it has important implications for climate change and natural hazards forecasting (Eichner et al. 2011; Sharma et al. 2012; Baranowski et al. 2015).

Processes exhibiting an exponential decay of its autocorrelation function $R(\tau)$ for large temporal intervals τ are known as short-range correlated processes, while those with a power-law decay, $R(\tau) \sim 1/\tau^{\gamma}$, are referred to as long-range correlated, long-range dependent, or long-memory processes. Accordingly, the power spectrum $S(f)$ of a stationary long-range correlated process exhibits a power-law behavior of the type $S(f) \sim 1/f^{\beta}$, with $\beta = 1 - \gamma$. This power-law scaling behavior, or scale invariance, underscores the lack of a single characteristic time scale dominating the dynamics of the underlying process. In other words, the existence of long-range correlation and scale invariance reveals similar statistical properties at different time scales, or equivalently the process exhibits statistical self-similarity or fractal structure, whereby the magnitude of short- and long-term fluctuations is related to each other through a single scale factor (Bassingthwaighte et al. 1994).

Fractal time series can be classified into two different groups. On the one hand, the scaling properties of one group are characterized by a single exponent, known as monofractals; on the other hand, those with much more complex patterns, known as multifractals, in which a continuous spectrum of exponents is needed for an adequate characterization of its scaling properties (Feder 1988; Barabasi and Stanley 1995; Kantelhardt et al. 2002). Most natural processes belong to the multifractal class (Pavlov and Anishchenko 2007). Furthermore, causes leading to multifractality can be a broad probability distribution for the values of the time series, or a result of different long-term correlations of small and large fluctuations (Kantelhardt et al. 2002).

Several methods have been used to explore the scaling properties of natural phenomena in terms of monofractal and multifractal behavior. These can be grouped basically into frequency domain methods, including approaches based on spectral and wavelet analysis (Box et al. 1970; Muzy et al. 1991; Abry et al. 1998); and time domain methods, based on the random walk theory, such as rescaled range analysis (R/S; Hurst 1951) or the detrended fluctuation analysis (DFA; Peng et al. 1994), and its multifractal generalization [multifractal detrended fluctuation analysis (MFDFA); Kantelhardt et al. 2002].

Even though the autocorrelation function is a natural estimator of the persistence, their use for estimating the scaling exponent can lead to misleading results when dealing with long time lags (Malamud and Turcotte 1999). Similarly, the estimation of its Fourier transform, the power spectrum, can be limited by statistical uncertainties (Talkner and Weber 2000). Accordingly, it has been observed that estimations of the scaling exponents based on the power spectrum are usually less stable and reliable than those provided by the DFA method (Matsoukas et al. 2000). Another important advantage of the DFA methodology is its capability to remove polynomial trends of different order (Hu et al. 2001).

Generally, observations of natural systems exhibit nonstationarities, such as periodicities and trends, which can lead to a false detection of long-range correlations that have to be removed from the stochastic components to estimate its correct scaling behavior. Hence, it is important to use methods capable of removing the effects of possible trends in the series, such as the DFA and MFDFA, which are well-established methods for determining the scaling of long-term correlation in

presence of polynomial trends (Kantelhardt et al. 2002; Bashan et al. 2008; Caraiani 2012).

As previously mentioned, the existence of a fractal structure has been recognized by examining time series coming from many different scientific fields. In particular, climatological and hydrological series exhibit persistence over a wide range of time scales (e.g., Pelletier and Turcottte 1997; Baranowski et al. 2015). However, a broad bibliographic review on the topic shows that oceanographic processes have received scant attention in comparison with other branches of Earth sciences, such as hydrology, seismology, and meteorology. Paradoxically, in an early review on the ubiquity of this behavior in astrophysics and many other branches of physics (Press 1978), ocean currents were identified as a process with a power spectrum exhibiting a scaling behavior, hence suggesting the presence of long-term dependence. Nevertheless, to the best of our knowledge, the only contribution exploring the fractal properties of ocean currents is due to Ashkenazy and Gildor (2009). These authors examined the existence of temporal long-range correlations in sea surface currents' time series measured in the northern Gulf of Eilat by using a high-frequency radar system, during one year with a 30-min time resolution. The use of a power spectrum and DFA methods allowed them to conclude that measured time series of sea surface currents exhibit a significant monofractal structure for time scales ranging between several hours and less than a month.

The aim of this study is to gain deeper insight into the time behavior of ocean currents, by exploring whether long experimental records of ocean current speed measured at intermediate and large depths exhibit a fractal structure, using for this purpose the DFA and MFDFA methods. Furthermore, the relative contribution of causes leading to multifractality is examined by applying these methodologies to modified versions of the original time series.

The rest of the paper is organized as follows: The main characteristics of experimental data used in the study, as well as the fundamentals of the detrended fluctuation analysis and multifractal detrended fluctuation analysis methods, are outlined in section 2. The results derived from the application of these methodologies to the measured speed ocean current datasets, as well as to the corresponding transformed time series, are discussed in section 3, and conclusions follow in section 4.

2. Data and methodology

a. Data

The analysis is based on time series of ocean current speed obtained at a single-point mooring on the Madeira Abyssal Plain, known as KIEL276 station. It is located west of Madeira in the northern Canary Basin at nominal location 33°N, 22°W. The measurements from 1980 to 2000 have been performed by the Institut für Meereskunde, Kiel, Germany—now the GEOMAR Helmholtz-Zentrum für Ozeanforschung Kiel—and since 2000 by the Leibniz Institute for Baltic Sea Research in Warnemünde, Germany. All data used in the study are accessible via the OceanSITES database. Analyzed time series have been registered by current meters placed at approximately 1000- and 3000-m depth, although mooring replacement for equipment maintenance commonly results in slight changes in depth.

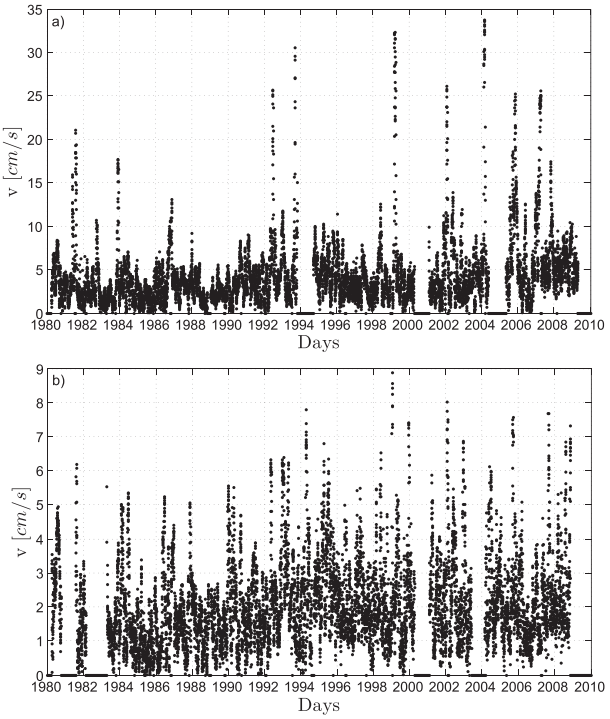

FIG. 1. Daily current speed time series recorded at (a) 1000- and (b) 3000-m depth.

Time series consist of daily averages of low-pass-filtered current speed measurements and cover a period of nearly 30 years, spanning from April 1980 to December 2009. Gaps of weeks—and in some cases months—are due to mooring or battery problems, instrument failures, etc.; thus, these discontinuities arise from the intrinsic nature of experimental recordings at sea. The percentage of missing data is around 15% and gaps are quite randomly distributed (see Fig. 1). A detailed description of the individual deployments is given in Müller and Waniek (2013), and further details together with a comprehensive analysis are given in Fründt et al. (2013). To deal with this kind of time series, a common preprocessing method is to cut out the

unreliable fragments and stitch together the remaining parts. This procedure is performed before executing any statistical analysis and, as it has already been proven, it does not have a significant impact on the scaling behavior of correlated signals—even when up to 50% of the points are removed (Chen et al. 2002).

b. Methodology

As previously stated, a compulsory step prior to any procedure for examining the presence of long-range correlations in a time series consists of removing trends and periodic patterns of variability associated with external effects. In particular, because natural time series generally exhibit a seasonal cycle, a deseasonalization procedure is performed by adjusting the data with the seasonal mean and standard deviation as $x = (x_i - x_d)/\sigma_d$, where x_i is the measured value of the current speed at day number i, during the recording period, with x_d and σ_d being the corresponding average and standard deviation for that particular day over the years, respectively (e.g., Livina et al. 2011).

1) Detrended fluctuation analysis

The DFA (Peng et al. 1994) transforms the autocorrelation function decay into an increasing variability measure. Then, a power law may be obtained that describes the magnitude of fluctuations as a function of the temporal scale and from which it is possible to infer a scaling behavior, if any.

As implied by its name, this method is based on the idea of detrending local variabilities—that is, external trends—that can be separated from the stochastic components of the time series. It is commonly denoted as DFA-p, indicating that polynomial trends of order p can be systematically fitted and eliminated to characterize quantitatively long-range correlations in nonstationary time series. In this study, several tests have been made by applying different orders of polynomial fits. Finally, it has been considered that it is sufficient to assume that the underlying process is mainly affected by linear trends, since the obtained scaling exponents did not show significant differences when removing polynomials of order up to three.

DFA methodology details can be found in Peng et al. (1994). In brief, this procedure can be described as follows: First, the original time series x is integrated to obtain the random walk profile enhancing self-similarity properties. It can be shown that original and integrated time series have both identical correlation structures (Lamperti 1962; Beran 1994; Willinger et al. 1997). The integrated time series is given by

$$y(k) = \sum_{i=1}^{k} [x(i) - \bar{x})] \quad k = 1, \ldots, N_b, \tag{1}$$

where $\bar{x}$ is the mean of the deseasonalized time series x and N is its length.

Next, the profile is divided into $N_b = N/n$ nonoverlapping segments, each containing n data points. To ensure a reliable estimation of the fluctuation function $F(n)$, n should not be larger than $N/4$ (Rybski et al. 2008). Each segment is locally detrended using a polynomial function y_p. The fluctuation function, which can be regarded as the variance of the detrended time series, is evaluated in each segment as

$$F_r(n) = \left[\frac{1}{n} \sum_{k=(r-1)n+1}^{rn} |y(k) - y_p(k)|^2 \right]^{1/2} \quad r = 1, \ldots, N_b. \tag{2}$$

Finally, by averaging $F_r(n)$ over the N_b intervals, the mean value of the fluctuation function is obtained. This procedure is repeated over different time scales, that is, n, to provide a relationship between $F(n)$ and n,

$$F(n) \sim n^H, \tag{3}$$

where H represents the Hurst exponent and quantifies the strength of the correlations. A linear relationship of $\log F(n)$ versus $\log(n)$ indicates self-similarity, and the slope of the regression line is effectively the scaling or Hurst exponent. Different types of behavior can be distinguished depending on its value. A slope of $H = 0.5$ corresponds to a process with no long-term correlations—that is, white noise or short-term memory—whereas $H = 1.5$ is related to an integrated random walk—that is, Brownian noise—which exhibits self-similarity but no long-range correlations. For $1/2 < H < 1$ there is persistence—that is, if in the immediate past the signal has a positive increment, then on average an increase of the signal in the immediate future is expected. On the contrary, $0 < H < 1/2$ implies antipersistence, meaning that an increasing value in the immediate past implies a decreasing in the immediate future. In the particular case of $H = 1$, temporal fluctuations are of flicker-noise type (i.e., $1/f$ noise), typical of self-organized criticality systems (Bak et al. 1987). However, this result could be also pointing to a process that is in essence multifractal and therefore more than one scaling exponent is required to fully characterize its dynamics (Beran 1994; Hausdorff and Peng 1996).

2) Multifractal detrended fluctuation analysis

As previously mentioned, multifractals are characterized by high variability on a wide range of temporal scales and the description of their scaling properties requires many scaling exponents. The MFDFA is a generalization of the DFA, based on the standard partition function

multifractal formalism for normalized and stationary measurements (Kantelhardt et al. 2002), which is useful for detecting the existence of distinct scaling behaviors at different time scales. By means of the MFDFA, the scaling of the qth-order moments of the fluctuation function are determined, instead of obtaining only the second-order statistical moment as in the case of the DFA. The procedure is similar to the previous one, with the difference that in this case Eq. (2) is rewritten as

$$F_{r,q}(n) = \left[\frac{1}{n}\sum_{k=(r-1)n+1}^{rn} |y(k) - y_p(k)|^{q/2}\right]^{1/2} \quad r = 1, \ldots, N_b. \tag{4}$$

Then, the fluctuation function of order q is obtained by averaging $F_{r,q}(n)$ over all the N_b segments,

$$F_q(n) = \frac{1}{N_b}\sum_{r=1}^{N_b} F_{r,q}(n). \tag{5}$$

The scaling exponent of each fluctuation function is calculated from log–log plots of $F_q(n)$ versus n for each value of q. Term $F_q(n)$ will generally increase for large values of n according to the following power law:

$$F_q(n) \sim n^{H_q}. \tag{6}$$

The exponent H_q, called the generalized Hurst exponent, describes the scaling behavior of the qth-order fluctuation function. For positive values of q, H_q characterizes segments with large fluctuations (small values of H_q), while negative values describe segments with small fluctuations (large values of H_q). Generally, q can take any real value. For $q = 2$, the standard DFA procedure is retrieved and $H_q = H$.

The generalized Hurst exponent is only one of several parameters used to characterize the multifractal structure of time series. There are other alternatives to describe this kind of series, such as the singularity spectrum $D(\alpha)$. Commonly, H_q is related to the classical multifractal scaling exponent—also known as the Renyi index τ_q, where $\tau_q = qH_q - 1$—and can be used to compute the singularity, or Hölder exponent α, via a Legendre transform (Feder 1988), by means of the following expression:

$$\alpha = \tau_q' = H_q + qH_q'. \tag{7}$$

Then, the singularity spectrum is obtained as

$$D(\alpha) = q\alpha - \tau_q = q(\alpha - H_q) + 1. \tag{8}$$

The plot of $D(\alpha)$ versus α, called the multifractal spectrum, typically has a parabolic concave downward shape, with the range of α values increasing with the process complexity. Its width ($\Delta\alpha = \alpha_{\max} - \alpha_{\min}$) represents deviations from the average fractal structure, given by the Hurst exponent derived from the monofractal analysis for large and small fluctuations. Then, it measures the degree of the series multifractality. If a spectrum has a nonsymmetric shape with one tail larger than the other one, then the larger tail is ignored and the width is estimated as the shorter tail doubled (Makoview and Fuliński 2010). For $q > 0$ the spectrum will have a long left tail when the time series has a multifractal behavior insensitive to local fluctuations with small magnitudes; on the other hand, for $q < 0$, the spectrum will have a long right tail when the time series has a multifractal behavior insensitive to local fluctuations with large magnitudes (Makoview et al. 2011).

Generally, the concept of generalized dimension $D(\alpha)$ corresponds to the scaling exponent for the qth moment of the measure. Thus, $D(\alpha)$ attains its maximum value ($D(\alpha) = 1$) for $q = 0$—see Eq. (8). For a monofractal, $D(\alpha)$ is a constant function of q, and no additional information is obtained by examining higher moments.

3) CONTRIBUTIONS TO MULTIFRACTALITY

It has been previously commented that it is possible to distinguish between two different contributions to multifractality: on the one hand, a linear contribution due to the existence of different long-term correlations of small and large fluctuations in the data; on the other hand, a nonlinear contribution as a consequence of a broad probability distribution (Kantelhardt et al. 2002; Schreiber and Schmitz 2000). Both effects are often present in real-world time series and can be individually eliminated to quantify the relative importance of each contribution on the scaling behavior. The methods commonly used to test the existence and relative importance of each type of multifractality are briefly described below.

(i) Shuffling

The shuffling method is a useful technique to quantify the strength of the linear contribution on the scaling properties of a process. Shuffled data are generated by random permutations of the original time series (Peters 1996). Random permutations guarantee the same amplitude distribution than the original series but destroy any temporal correlations between observations. Hence, shuffled versions of series with multifractality due to only long-range correlations for small and large fluctuations will exhibit a simple white noise behavior. However, this procedure does not affect multifractal contribution due to probability density broadness. When both types of multifractality are present,

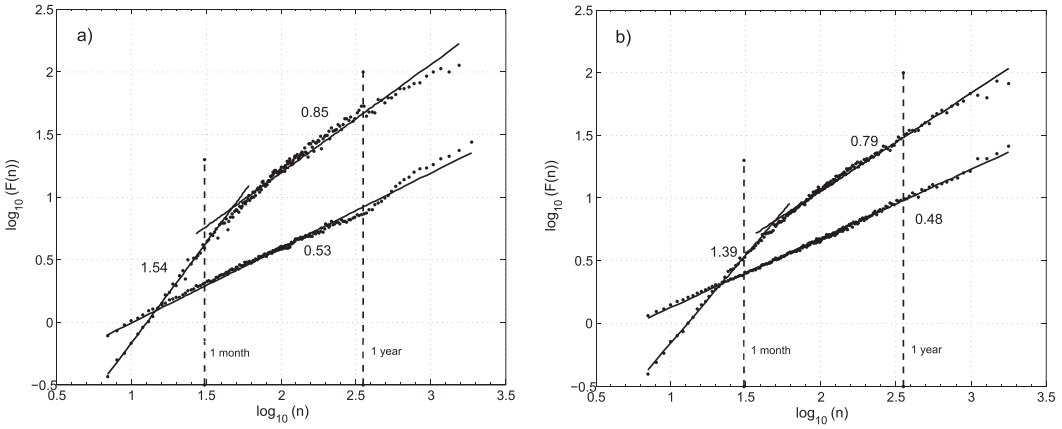

FIG. 2. Log–log plots of the fluctuation function vs the scale (days) of the original and shuffled time series at (a) 1000- and (b) 3000-m depth. Solid lines represent least squares fitted lines.

multifractality of the original series will be stronger than that of its shuffled versions.

(ii) Surrogate data

Generation of surrogate data has been suggested as a procedure for testing the existence of nonlinearities in time series (Theiler et al. 1992). The tests are based on the generation of synthetic time series, denoted as surrogate series, which preserve some statistical characteristics of the original, or tested, time series, but randomize the Fourier phases and hence remove nonlinearities. There are several algorithms for generating surrogate time series. The procedure used in this study is known as iterative amplitude-adjusted Fourier transform (IAAFT) and enables synthesizing time series in which nonlinearities present in the original time series are removed while preserving its power spectrum and probability distribution (Schreiber and Schmitz 1996).

(iii) Volatility time series

An additional technique to evaluate the nonlinearity degree on the scaling properties of a process consists of studying the correlations of the volatility time series (Kalisky et al. 2005). Volatility is defined as the absolute values of the increment of the original data $\Delta x_i = |x_{i+1} - x_i|$ (Liu et al. 1999). It has already been shown that long-range correlations in volatility time series are related to multifractality and in particular to the nonlinearity characteristics of a process (Ashkenazy et al. 2003). Thus, volatility time series derived from nonlinear and long correlated records exhibit long correlations too, according to a monofractal analysis. On the contrary, if the original data are completely linear and present long-range correlations, then their volatility time series will not show long-range correlations.

3. Results and discussion

Time series of daily current speed at 1000- and 3000-m depth are shown in Figs. 1a and 1b, respectively. As expected (e.g., Talley et al. 2011), the strength and range of variability of current speed are significantly smaller at 3000-m depth. Thus, a simple statistical data analysis reveals a clear decrease with depth of the mean and standard deviation of current speed—4.23 $\pm$3.73 cm s^{-1} (1000 m) and 2.06 $\pm$ 1.28 cm s^{-1} (3000 m)—as well as a drastic reduction of the range of variability, from 0 to nearly 34 cm s^{-1} at 3000 m and between 0 and 9 cm s^{-1} at 1000 m, approximately. These differences are mainly due to strong episodic current events detected at 1000-m depth, with speeds exceeding 15 and even 30 cm s^{-1}.

a. Monofractal analysis

The log–log plots of the DFA function versus time scale in days, for the original and shuffled current speed records at 1000- and 3000-m depth, are shown in Figs. 2a and 2b, respectively. It is quite clear from these figures that at both depths there exists a crossover point that separates the time-scale range into two subbands with different power-law behaviors. The scaling exponents associated with each band have been estimated as the slope of the straight line fitted to the data by means of the least squares method at each side of the crossover point.

It can be observed that for time scales larger than approximately 5 years, both fits deviate from the scaling behavior, exhibiting an increasing dispersion. In this sense, it is important to take into account that the number of segments used to obtain the average value of $F(n)$ decreases as n increases and, consequently, the statistical stability of these estimations reduces. Accordingly, the discussion on the scaling behavior is

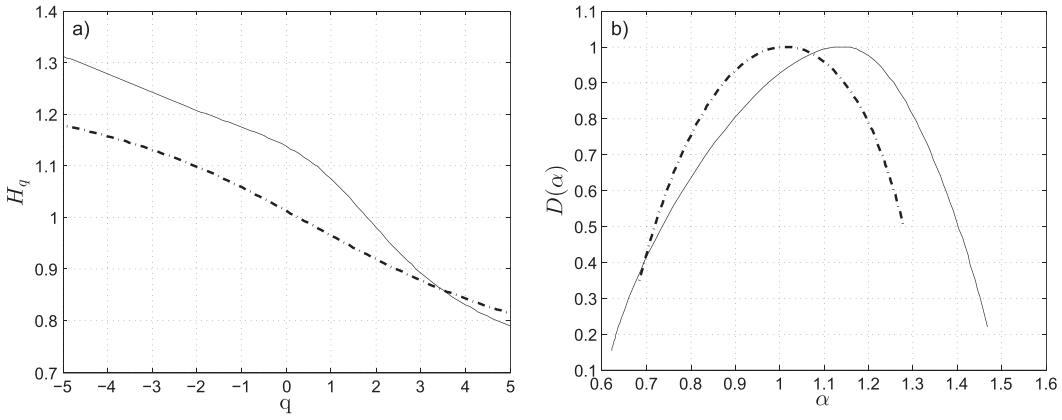

FIG. 3. Generalized Hurst exponent as a function of q for (a) current speed time series at 1000- (solid line) and 3000-m depth (dashed line), and (b) multifractal spectra for 1000- (solid line) and 3000-m depth (dashed line).

limited to time scales below 5 years, where the data adequately conform to a straight line.

Crossovers are located at time points close to 50 days at both depths. Thus, fluctuations of current speed at time scales between approximately 50 days and 5 years exhibit long-range correlations with scaling exponents equal to 0.85 and 0.79 for 1000 and 3000 m, respectively. The corresponding scaling exponents for shorter time scales are 1.54 and 1.39, implying a Brownian motion–type behavior (Peng et al. 1994).

The appearance of crossovers in the curves derived through DFA seems to be a common feature of geophysical time series. In particular, Monetti et al. (2003) studied the persistence of the sea surface temperature and found two different scaling behaviors for time scales below and above 10 months. Moreover, Livina et al. (2011) observed the existence of a crossover at a few months' scale when exploring long-term correlations in river flux data, a variable closely related to current speed. Nevertheless, careful consideration should be given to the presence of crossovers, since they may not be reflecting different behaviors at different temporal scales, but an effect of trends embedded in the time series (Hu et al. 2001). Other nonstationarities can also cause crossovers if they are not properly taken into account, such as seasonal variations (Livina et al. 2011). Moreover, it has to be stressed that crossovers must not be confused with multifractality, since multifractality is characterized by different scaling behaviors of different moments over the full range of time scales (Bouchaud et al. 2000).

Another point to mention is the decrease of H as the distance from the sea surface increases. This is probably related to the change in the number of involved physical processes operating at different time scales, which is higher at 1000-m depth than at 3000-m depth. In this regard, it is interesting to note that, although the dynamics of surface ocean currents are substantially different from that of deep ocean currents, Ashkenazy and Gildor (2009), when analyzing long-range correlations of ocean surface currents in a semienclosed sea, obtain similar scaling exponents as the ones obtained in the present study in the scale range above approximately 50 days. Nevertheless, the temporal scale range examined by these authors is between a few hours and less than one month, which is well below the time scales considered in this study.

Application of DFA to the corresponding shuffled time series at 1000- and 3000-m depth results in a sole scaling exponent close to 0.5 in both cases, as depicted in Fig. 2. This reveals that by randomizing the original time series, long-range dependence disappears, implying that the scaling behavior of current speed fluctuations is mainly dominated by temporal correlations.

The predominance of long-range correlations in the process and the reduction of their strength with depth agrees with the existence of events during which current speed reaches extreme values somewhat clustered in time, as seen in Fig. 1, especially at 1000-m depth (Fig. 1a).

b. *Multifractal analysis*

As discussed in the previous section, most natural records do not exhibit a simple monofractal scaling behavior. Therefore, a multifractal analysis is performed to determine whether the current speed time series requires more than one exponent for a full description of its scaling behavior in the same range of time scales.

The dependence of H_q with q is shown in Fig. 3a. It can be observed that H_q decreases monotonically with the increase of q, revealing a different scaling behavior for small and large fluctuations of current speeds, and suggesting that the deep current speed time series exhibits multifractal characteristics at both depths. For a

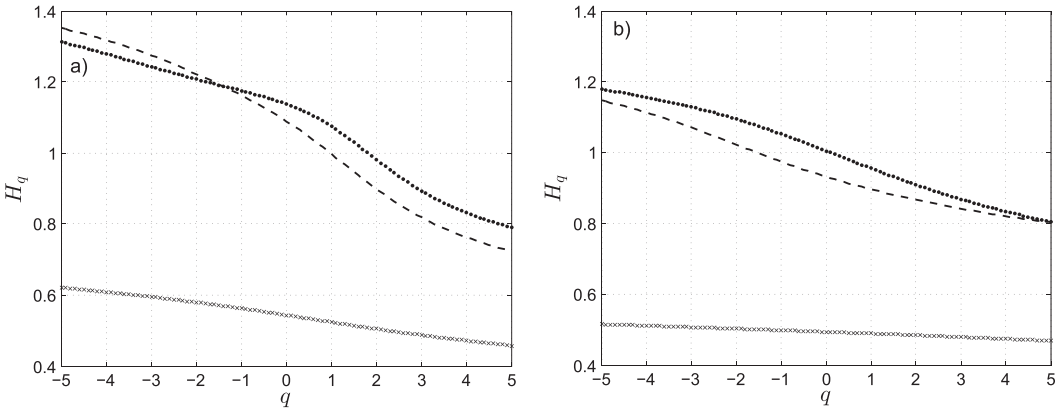

FIG. 4. Generalized Hurst exponent as a function of q for the original (dotted line), shuffled (crossed line), and surrogated (dashed line) current speed time series at (a) 1000- and (b) 3000-m depth.

monofractal time series, H_q is independent of q. Hence, the rate of change of H_q can be used as a measure for the strength of the multifractal character of a process. Accordingly, the multifractality degree decreases with depth. Furthermore, the decreasing pattern of H_q with q is more nonlinear for currents at 1000 than at 3000 m, indicating a larger difference in the scaling of small ($q < 0$) and large fluctuations ($q > 0$) in the upper point of measure.

Another useful way of characterizing the multifractal behavior of a process is by means of $D(\alpha)$, derived from H_q [Eq. (8)]. This quantifies in detail the long-range correlation properties of a time series (Ashkenazy et al. 2003). In particular, the $\Delta\alpha$ of multifractal spectra constitutes a measure of the multifractality degree. Theoretically, for a monofractal time series the multifractal spectrum reduces to a single point. Thus, the wider the $\Delta\alpha$, the stronger the multifractality will be, and the more complex the process from which the time series derive.

Multifractal spectra of current speed time series at 1000- and 3000-m depth are shown in Fig. 3b. It is remarkable that in both cases the spectrum exhibits a typical parabolic concave downward shape, indicating a multifractal structure at both depths. The location of the maxima varies with depth, peaking around $\alpha \sim 1.14$ and $\alpha \sim 1.08$ at 1000 and 3000 m, respectively. These values are close to the mean value of the scaling exponents obtained in the DFA, suggesting that the maximum of the multifractal spectrum gives insight into the dominant scaling behavior.

Concerning the width of $D(\alpha)$, it is observed how it decreases as the depth increases. Thus, the complexity degree is higher at 1000 m, with $\Delta\alpha \sim 0.66$, than at 3000 m, where $\Delta\alpha \sim 0.4$. This fact also manifests itself in the generalized Hurst exponent variation range (Fig. 3a), which is clearly larger for 1000 m, varying from around 1.35 to 0.78. It can also be noticed that at 1000-m depth, the spectrum is slightly skewed to the right, which indicates relatively strongly weighted high fractal exponents (Shimizu et al. 2002), and regarding its tails, the current speed time series seems to have a multifractal structure mainly dominated by long-range fluctuations.

The variation of multifractality with depth suggests a different specific influence of the two factors contributing to the multifractal structure of the observed time series. To corroborate this point, the DFA and MFDFA methods have been applied to shuffled, surrogate, and volatility time series associated with the original one. If the order of observations in a multifractal time series is randomly modified, then its memory component is removed and some part of its multifractality should disappear, resulting in a narrower multifractal spectrum. On the other hand, most of the remaining multifractality should disappear if nonlinearities present in the time series are eliminated by randomizing the corresponding Fourier phases. Thus, the relative reduction in width of the multifractal spectrum generated by the shuffling and phase-randomization procedures provides information on the specific importance of the linear and nonlinear contributions to the observed degree of multifractality.

The variations of the generalized Hurst exponent with q are shown in Fig. 4a for the current speed time series at 1000 m and in Fig. 4b for 3000-m depth. Note that the range of H_q values reduces drastically for the shuffled time series, being almost independent of q and close to 0.5 at both depths. The slope of H_q around $q = 0$ reduces for the surrogate time series and reaches even lower values for shuffled versions. This fact is particularly true for currents at 3000-m depth. These results indicate that multifractality is mainly caused by different long-range temporal correlations for small and large fluctuations, while the effect of the fat-tailed distribution is almost

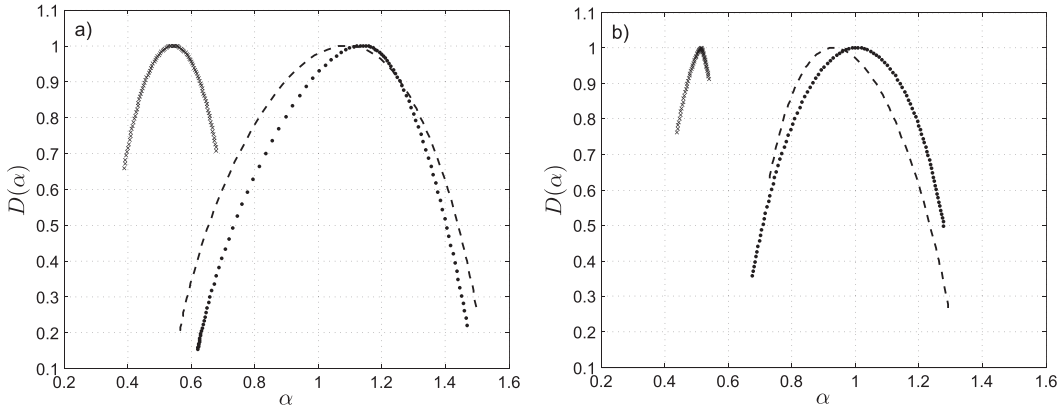

FIG. 5. Multifractal spectra for current speed at (a) 1000- and (b) 3000-m depth. Dotted, crossed, and dashed lines correspond to spectra of the original, shuffled, and surrogated time series, respectively.

negligible at the lower depth and weak at the more superficial point of measurement. Furthermore, some nonnegligible differences can be observed in the relationship of H_q with q, particularly for $q > 0$, for the original and surrogated time series at 1000-m depth, which hints at the existence of nonlinear contributions affecting the scaling behavior of large fluctuations.

Additional support for these findings can be obtained by exploring changes in the structure and location of the multifractal spectrum of the original and modified time series. For this purpose, multifractal spectra associated with original, shuffled, and surrogate time series are shown for current speeds recorded at 1000- and 3000-m depth in Figs. 5a and 5b, respectively. It can be observed that the width of the shuffled time series spectra decreases significantly and that the location of their maxima shifts toward 0.5 (approaching the behavior of a white noise), with regard to that of the original series. However, these effects are almost negligible for the surrogated time series multifractal spectra, mainly at 3000-m depth, indicating possible nonlinear contributions in the observations recorded at 1000-m depth.

To test and provide extra support to this fact, the scaling properties of the volatility time series derived from each current speed record are examined. A comparison of DFA results for volatility time series and their corresponding surrogate versions shows a slight decrease of the scaling exponent for the surrogate volatility series ($H_v = 0.82$ and $H_{v-s} = 0.76$, respectively) at 1000-m depth (Fig. 6a), while the exponent remains constant, $H_v = H_{v-s} \approx 0.74$, at 3000-m depth (Fig. 6a), endorsing the idea of some weak nonlinear contribution to the fractal characteristics of the speed time series measured at 1000-m depth. In this context, it is interesting to note that Ashkenazy and Gildor (2009) performed a similar analysis for volatility sea surface current speed time series and identified a significant nonlinear contribution to the fractal structure of the process.

On the basis of the findings above, it seems reasonable to admit a decrease in the multifractality, and hence the

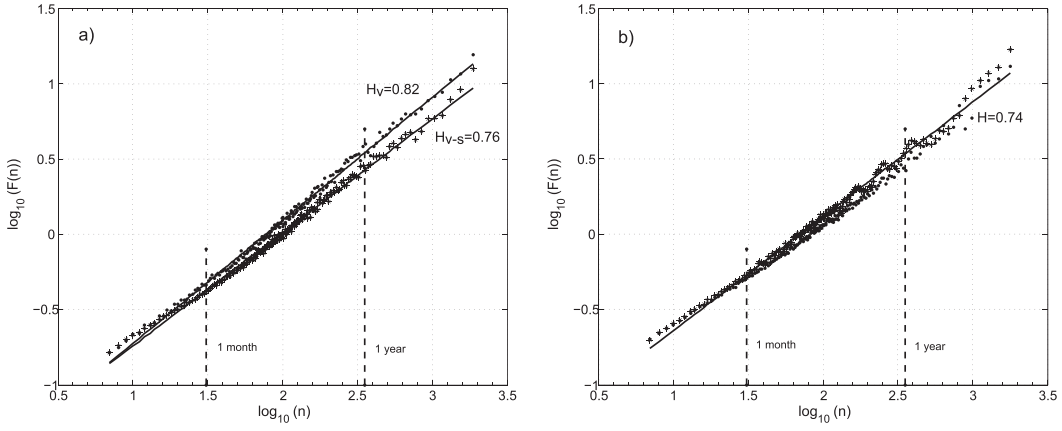

FIG. 6. DFA for volatility and surrogated volatility current speed time series at (a) 1000- and (b) 3000-m depth.

complexity, of the ocean current speed time series, as well as a decreasing relative importance of the nonlinear contribution associated with the fat-tailness of the probability density function, as the depth increases. These results can be, at least partially, explained by the reduction with depth in the number of physical processes operating at different time scales and giving rise to the observed ocean current speed time series.

4. Conclusions

Fractal properties of deep ocean current speed time series recorded at two different depths, 1000 and 3000 m, are investigated by using the DFA and MFDFA methods. The monofractal analysis methodology reveals that analyzed ocean current speed time series exhibit power-law behavior in the time-scale range between one week and 5 years. The presence of a crossover located around 50 days, at both depths, divides this range into two subbands with different scaling exponents. Time scales larger than 50 days exhibit long-range correlations, while shorter time scales are characterized by a Brownian motion–type behavior, at both depths. In both subranges the scaling exponent decreases as the depth increases. Furthermore, the application of the DFA method to shuffled time series at both depths reveals the dominance of temporal correlations on the scaling behavior of current speed fluctuations.

Multifractal analysis reveals that current speed time series at both depths do not exhibit a simple fractal structure but have a multifractal nature whose strength decreases with depth. The analysis of shuffled and Fourier phase randomized versions of the original time series demonstrates that the multifractal structure is mainly due to different long-range temporal correlations for small and large fluctuations at both depths, but it also indicates the existence of some weak nonlinear contribution, due to the fat-tailness of the probability distribution, to the multifractality at 1000-m depth, which practically disappears at 3000-m depth. This fact is reinforced by results from the detrended fluctuation analysis of volatility time series.

Acknowledgments. We gratefully acknowledge the financial support by Deutsche Forschungsgemeinschaft (DFG) over many years in a variety of grants to different German institutions and individuals involved in the work at the site KIEL 276. We thank the masters, crews, and scientists who assisted and supported the work during numerous sampling campaigns aboard a number of German research vessels. Our special thanks are directed to the masters and crews of R/V *Poseidon*, as most of the recent cruises were carried out on board this ship. JW acknowledges also the Leibniz Institute for Baltic Sea Warnemunde for the occasional financial support in recent years. We also thank the two anonymous reviewers, whose comments and suggestions helped us to improve the first version of the manuscript.

REFERENCES

Abry, P., D. Veitch, and P. Flandrin, 1998: Long-range dependent: Revisiting aggregation with wavelets. *J. Time Ser. Anal.*, **19**, 253–266, doi:10.1111/1467-9892.00090.

Ashkenazy, Y., and H. Gildor, 2009: Long-range temporal correlations of ocean surface currents. *J. Geophys. Res.*, **114**, C09009, doi:10.1029/2008JC005235.

——, S. Havlin, P. Ivanov, C.-K. Peng, V. Shulte-Frohlinde, and H. Stanley, 2003: Magnitude and sign scaling in power-law correlated time series. *Physica A*, **323**, 19–41, doi:10.1016/S0378-4371(03)00008-6.

Bak, P., C. Tang, and K. Wiesenfeld, 1987: Self-organized criticality: An explanation of 1/*f* noise. *Phys. Rev. Lett.*, **59**, 381, doi:10.1103/PhysRevLett.59.381.

Barabasi, A., and H. Stanley, 1995: *Fractal Concepts in Surface Growth.* University Press, 369 pp.

Baranowski, P., J. Krzyszczak, C. Slawinski, H. Hoffmann, J. Kozyra, A. Nierobca, K. Siwek, and A. Gluza, 2015: Multifractal analysis of meteorological time series to assess climate impacts. *Climate Res.*, **65**, 39–52, doi:10.3354/cr01321.

Barbosa, S., M. Fernandes, and M. Silva, 2006: Long-range dependence in North Atlantic sea level. *Physica A*, **371**, 725–731, doi:10.1016/j.physa.2006.03.046.

Bashan, A., R. Bartsch, J. Kantelhardt, and S. Havlin, 2008: Comparison of detrending methods for fluctuation analysis. *Physica A*, **387**, 5080–5090, doi:10.1016/j.physa.2008.04.023.

Bassingthwaighte, J., L. Liebovitch, and B. West, 1994: *Fractal Physiology.* Oxford University Press, 355 pp.

Beran, J., 1994: *Statistics for Long Memory Processes.* Chapman and Hall, 320 pp.

Bouchaud, J., M. Potters, and M. Meyer, 2000: Apparent multifractality in financial time series. *Eur. Phys. J.* **13B**, 595–599.

Box, G., G. Jenkins, and G. Reinsel, 1970: *Time Series Analysis: Forecasting and Control.* J. Wiley and Sons, 729 pp.

Bunde, A., and S. Lennartz, 2012: Long-term correlations in earth sciences. *Acta Geophys.*, **60**, 562–588, doi:10.2478/s11600-012-0034-8.

Caraiani, P., 2012: Evidence of multifractality from emerging European stock markets. *PLoS One*, **7**, e40693, doi:10.1371/journal.pone.0040693.

Chen, Z., P. Ivanov, K. Hu, and H. E. Stanley, 2002: Effect of nonstationarities on detrended fluctuation analysis. *Phys. Rev.*, **65E**, 041107, doi:10.1103/PhysRevE.65.041107.

Eichner, J., J. Kantelhardt, A. Bunde, and S. Havlin, 2011: The statistics of return intervals, maxima, and centennial events under the influence of long-term correlations. *In Extremis: Disruptive Events and Trends in Climate and Hydrology*, J. Kropp, and H.-J. Schellnhuber, Eds., Springer, 2–43, doi:10.1007/978-3-642-14863-7_1.

Feder, J., 1988: *Fractals.* Plenum Press, 243 pp.

Fründt, B., T. Müller, E. Schulz-Bull, and J. Waniek, 2013: Long-term changes in the thermocline of the subtropical Northeast Atlantic (33°N, 22°W). *Prog. Oceanogr.*, **116**, 246–260, doi:10.1016/j.pocean.2013.07.004.

Goldberger, A., L. Amaral, J. Hausdorff, P. Ivanov, C.-K. Peng, and H. E. Stanley, 2002: Fractal dynamics in physiology:

Alterations with disease and aging. *Proc. Natl. Acad. Sci. USA*, **99**, 2466–2472, doi:10.1073/pnas.012579499.

Hausdorff, J., and C. Peng, 1996: Multiscaled randomness: A possible source of 1/*f* noise in biology. *Phys. Rev.*, **54E**, 2154, doi:10.1103/PhysRevE.54.2154.

Hu, K., P. Ivanov, Z. Chen, P. Carpena, and H. E. Stanley, 2001: Effect of trends on detrended fluctuation analysis. *Phys. Rev.*, **64E**, 011114, doi:10.1103/PhysRevE.64.011114.

Huang, R., 2010: *Ocean Circulation: Wind-Driven and Thermohaline Processes.* Cambridge University Press, 791 pp.

Hurst, H., 1951: Long-term storage capacity of reservoirs. *Trans. Amer. Soc. Civ. Eng.*, **116**, 770–799.

Huybers, P., and W. Curry, 2006: Links between annual, Milankovitch and continuum temperature variability. *Nature*, **441**, 329–332, doi:10.1038/nature04745.

Kalisky, T., Y. Ashkenazy, and S. Havlin, 2005: Volatility of linear and nonlinear time series. *Phys. Rev.*, **72E**, 011913, doi:10.1103/PhysRevE.72.011913.

Kantelhardt, J., S. Zschiegner, E. Koscielny-Bunde, S. Havlin, A. Bunde, and H. E. Stanley, 2002: Multifractal detrended fluctuation analysis of nonstationary time series. *Physica A*, **316**, 87–114, doi:10.1016/S0378-4371(02)01383-3.

——, D. Rybski, S. Zschiegner, P. Braun, E. Koscielny-Bunde, V. Livina, S. Havlin, and A. Bunde, 2003: Multifractality of river runoff and precipitation: Comparison of fluctuation analysis and wavelet methods. *Physica A*, **330**, 240–245, doi:10.1016/j.physa.2003.08.019.

Lamperti, J., 1962: Semi-stable stochastic processes. *Trans. Amer. Math. Soc.*, **104**, 62–78, doi:10.1090/S0002-9947-1962-0138128-7.

Liu, Y., P. Gopikrishnan, P. Cizeau, M. Meyer, C. Peng, and H. E. Stanley, 1999: Statistical properties of the volatility of price fluctuations. *Phys. Rev.*, **60E**, 1390, doi:10.1103/PhysRevE.60.1390.

Livina, V., Z. Kizner, P. Braun, T. Molnar, A. Bunde, and S. Havlin, 2007: Temporal scaling comparison of real hydrological data and model runoff records. *J. Hydrol.*, **336**, 186–198, doi:10.1016/j.jhydrol.2007.01.014.

——, Y. Ashkenazy, A. Bunde, and S. Havlin, 2011: Seasonality effects on nonlinear properties of hydrometeorological records. *In Extremis: Disruptive Events and Trends in Climate and Hydrology*, J. Kropp and H.-J. Schellnhuber, Eds., Springer, 266–284, doi:10.1007/978-3-642-14863-7_13.

Makoview, D., and A. Fuliński, 2010: Multifractal detrended fluctuation analysis as the estimator of long-range dependence. *Acta Phys. Pol.*, **41B**, 1025–1049.

——, A. Rynkiewicz, R. Gałąska, J. Wdowczyk-Szulc, and M. Żarczyńska-Buchowiecka, 2011: Reading multifractal spectra: Aging by multifractal analysis of heart rate. *Europhys. Lett.*, **94**, 68005, doi:10.1209/0295-5075/94/68005.

Malamud, R., and D. Turcotte, 1999: Self-affine time series: Measures of weak and strong persistence. *J. Stat. Plann. Inference*, **80**, 173–196, doi:10.1016/S0378-3758(98)00249-3.

Mandelbrot, B. B., and J. R. Wallis, 1969: Some long-run properties of geophysical records. *Water Resour. Res.*, **5**, 321–340, doi:10.1029/WR005i002p00321.

Mantegna, R., and H. Stanley, 1995: Scaling behavior in the dynamics of an economic index. *Nature*, **376**, 46–49, doi:10.1038/376046a0.

Matsoukas, C., S. Islam, and I. Rodriguez-Iturbe, 2000: Detrended fluctuation analysis of rainfall and streamflow time series. *J. Geophys. Res.*, **105**, 29 165–29 172, doi:10.1029/2000JD900419.

Monetti, R., S. Havlin, and A. Bunde, 2003: Long-term persistence in the sea surface temperature fluctuations. *Physica A*, **320**, 581–589, doi:10.1016/S0378-4371(02)01662-X.

Müller, T., and J. Waniek, 2013: KIEL276 time series data from moored current meters. GEOMAR Helmholtz-Zentrum für Ozeanforschung Kiel Rep. 13, 239 pp.

Muzy, J., E. Bacry, and A. Arneodo, 1991: Wavelets and multifractal formalism for singular signals: Application to turbulence data. *Phys. Rev. Lett.*, **67**, 3515–3518, doi:10.1103/PhysRevLett.67.3515.

Pavlov, A. N., and V. S. Anishchenko, 2007: Multifractal analysis of complex signals. *Phys.-Usp.*, **50**, 819, doi:10.1070/PU2007v050n08ABEH006116.

Pelletier, J., and D. Turcottte, 1997: Long-range persistence in climatological and hydrological time series: Analysis, modeling and application to drought hazard assessment. *J. Hydrol.*, **203**, 198–208, doi:10.1016/S0022-1694(97)00102-9.

Peng, C.-K., S. V. Buldyrev, S. Havlin, M. Simons, H. E. Stanley, and A. L. Goldberger, 1994: Mosaic organization of DNA nucleotides. *Phys. Rev.*, **49E**, 1685, doi:10.1103/PhysRevE.49.1685.

Peters, E., 1996: *Chaos and Order in the Capital Markets.* Wiley and Sons, 277 pp.

Pinet, P., 2009: *Invitation to Oceanography.* Jones and Bartlett, 613 pp.

Press, W. H., 1978: Flicker noises in astronomy and elsewhere. *Comment. Astrophys.*, **7**, 103–119.

Rybski, D., A. Bunde, and H. von Storch, 2008: Long-term memory in 1000-year simulated temperature records. *J. Geophys. Res.*, **113**, D02106, doi:10.1029/2007JD008568.

Schreiber, T., and A. Schmitz, 1996: Improved surrogate data for nonlinearity tests. *Phys. Rev. Lett.*, **77**, 635–638, doi:10.1103/PhysRevLett.77.635.

——, and ——, 2000: Surrogate time series. *Physica D*, **142**, 346–382, doi:10.1016/S0167-2789(00)00043-9.

Sharma, A., and Coauthors, 2012: Complexity and extreme events in geosciences: An overview. *Extreme Events and Natural Hazards: The Complexity Perspective, Geophys. Monogr.*, Vol. 196, Amer. Geophys. Union, 1–16, doi:10.1029/2012GM001233.

Shimizu, Y., S. Thurner, and K. Ehrenberger, 2002: Multifractal spectra as a measure of complexity in human posture. *Fractals*, **10**, 103–116, doi:10.1142/S0218348X02001130.

Stewart, R., 2009: *Introduction to Physical Oceanography.* Orange Grove Texts Plus, 354 pp.

Talkner, P., and R. Weber, 2000: Power spectrum and detrended fluctuation analysis: Application to daily temperatures. *Phys. Rev.*, **62E**, 150, doi:10.1103/PhysRevE.62.150.

Talley, L., G. Pickard, W. J. Emery, and J. Swift, 2011: *Descriptive Physical Oceanography: An Introduction.* Elsevier, 555 pp.

Taqqu, M., V. Teverovsky, and W. Willinger, 1997: Is network traffic self-similar or multifractal? *Fractals*, **5**, 63, doi:10.1142/S0218348X97000073.

Theiler, J., S. Eubank, A. Longtin, B. Galdrikian, and J. Farmer, 1992: Testing for nonlinearity in time series: The method of surrogate data. *Physica D*, **58**, 77–94, doi:10.1016/0167-2789(92)90102-S.

van Aken, H., 2007: *The Oceanic Thermohaline Circulation: An Introduction.* Springer Science and Business Media, 326 pp.

Willinger, W., M. Taqqu, W. Sherman, and D. Wilson, 1997: Self-similarity through high variability: Statistical analysis of Ethernet LAN traffic at the source level. *IEEE/ACM Trans. Networking*, **5**, 71–86, doi:10.1109/90.554723.